BIOCHEMISTRY

 Volume 46, Number 31 August 7, 2007

Articles

A Complex of Catalytically Inactive Protein Phosphatase-1 Sandwiched between Sds22 and Inhibitor-3†

Bart Lesage,‡ Monique Beullens,*,‡ Leda Pedelini,§ Maria Adelaida Garcia-Gimeno,§ Etienne Waelkens,‡ Pascual Sanz,§ and Mathieu Bollen‡

Laboratory of Biosignaling and Therapeutics, Department of Molecular Cell Biology, Faculty of Medicine, Catholic University of Leuven, B-3000 Leuven, Belgium, and Instituto de Biomedicina de Valencia (CSIC), Jaime Roig 11, 46010 Valencia, Spain

Received February 14, 2007; Revised Manuscript Received May 24, 2007

ABSTRACT: Protein Ser/Thr phosphatase-1 (PP1) associates with a host of proteins to form substrate-specific holoenzymes. Sds22 and Inhibitor-3 (I3) are two independently described ancient interactors of PP1. We show here by various approaches that Sds22 and I3 form a heterotrimeric complex with PP1, both in cell lysates and after purification. The stability of the complex depended on functional PP1 interaction sites in Sds22 and I3, indicating that PP1 is sandwiched between Sds22 and I3. Intriguingly, I3 could not be replaced in this complex by another PP1 interactor with the same PP1 binding motif. In vitro, Sds22 and I3 were potent inhibitors of PP1, but with only some substrates. The inhibition by Sds22 could be reproduced with synthetic Sds22 fragments comprising leucine-rich repeats (LRR) 2 and 5. Sds22 and LRR5 also slowly converted PP1 into a conformation that was inactive with all tested substrates. Cell lysates that were prepared under conditions that prevented the Sds22-induced inactivation of PP1 contained a catalytically inactive complex of Sds22, PP1, and I3, indicating that this complex exists in vivo. Therefore, our studies show that a pool of PP1 is complexly controlled by both Sds22 and I3.

Protein phosphatase-1 (PP1)[1] ranks among the most conserved eukaryotic proteins. It is a major protein Ser/Thr phosphatase that controls numerous cellular processes by the dephosphorylation of key regulatory proteins. Mammalian genomes harbor only three genes that encode isoforms of the catalytic subunit of PP1. However, these catalytic subunits interact with dozens of structurally unrelated proteins to form distinct holoenzymes with a well-defined localization and substrate specificity (*1*, *2*). PP2A, another major protein Ser/Thr phosphatase, shows a similar diversity at the holoenzyme level (*3*). This suggests that the diversification of protein Ser/Thr phosphatases during evolution can be largely attributed to an increase in the number of interacting proteins that determine when and where the

† This work was financially supported by the Fund for Scientific Research-Flanders (Grant G.0290.05), a Flemish Concerted Research Action, and the Prime Minister's office (IAP/V-05) to M. Bollen. A grant from the Spanish Ministry of Education and Science (Grant SAF-2005-00852) and a grant from the Instituto de Salud Carlos III (PI050423) to P.S. are also acknowledged.

* To whom correspondence should be addressed: Laboratory of Biosignaling and Therapeutics, Campus Gasthuisberg, O&N1 Box 901, Catholic University of Leuven, Herestraat 49, B-3000 Leuven, Belgium. Phone: +32-16-33 02 47. Fax: +32-16-34 59 95. E-mail: Monique.Beullens@med.kuleuven.be.

‡ Catholic University of Leuven.

§ Instituto de Biomedicina de Valencia.

[1] Abbreviations: I2, Inhibitor-2; I3, Inhibitor-3; NIPP1, nuclear inhibitor of PP1; PBS, phosphate-buffered saline; PP1, protein phosphatase-1; Sds22, suppressor 2 of dis2-11 mutation.

10.1021/bi7003119 CCC: $37.00
Published on Web 07/14/2007

phosphatase acts. On the other hand, protein Ser/Thr kinases appear to have used a different diversification strategy, largely based on a gradual increase in the number of catalytic subunits. Thus, in spite of the huge difference in the number of catalytic subunits of mammalian protein Ser/Thr kinases (ca. 400) and phosphatases (ca. 30), the number of holoenzymes for these two classes of enzymes may be more or less balanced (*1*, *2*).

There are already close to 100 mammalian proteins known to interact with PP1. These PP1-interacting proteins function as inhibitors, substrate specifiers, and/or substrate-targeting proteins. Sometimes, PP1 interactors are themselves substrates for associated PP1 (*1*). The two most ancient interactors of PP1 are Sds22 and Inhibitor-3 (I3), which originated during the divergence of the four supertaxa that constitute the eukaryotic crown (*4*). Sds22 and I3 are expressed in virtually all eukaryotes, including *Saccharomyces cerevisiae*, where the orthologues are known as Sds22 (*5*, *6*) and Ypi1 (*7*), respectively. The conservation of Sds22 and I3 over such a long evolutionary distance strongly indicates that these proteins fulfill an essential function in one or several basic cellular processes. Consistent with this notion, it was reported that the conditional loss of either Sds22 or Ypi1 in yeast is associated with an alteration of the nuclear localization of PP1 and cell growth arrest in midmitosis with an aberrant mitotic spindle (*8*, *9*). These results suggested a common role of these two proteins in the regulation of yeast PP1 (Glc7) nuclear function. Since a loss-of-function mutation of the Aurora-related yeast protein kinase Ipl1 could be relieved by the expression of mutant versions of Sds22 or PP1, it has been proposed that Sds22-associated PP1 acts antagonistically to Ipl1 (*8*, *10*). However, this contrasts with a more recent study that identified Sds22 as an Ipl1 dosage suppressor (*10*). These paradoxal findings can be rationalized by a putative function of Sds22 as a chaperone for PP1. According to this view, a loss of Sds22 would relieve the Ipl1 mutant phenotype because Sds22 is required in producing somehow functional PP1, which dephosphorylates Ipl1 substrates, and the loss of Sds22 would therefore keep Ipl1 substrates phosphorylated. Conversely, an excess of Sds22 would suppress the Ipl1 mutant phenotype because it titrates PP1 away from its Ipl1 substrates. Recently, Pedelini et al. (*9*) have also described that the overexpression of Ypi1 is able to rescue the Ipl1 mutant phenotype.

Sds22 largely consists of 11 leucine-rich repeats (LRR), each of which forms a hairpinlike conformation and assembles into a curved superhelix. The C-terminus of Sds22 was proposed to function as a LRR cap structure that shields the hydrophobic core of the LRRs from solvent. A bipartite interaction site for PP1 was mapped to the concave site of the LRR superhelix. Sds22 binds to the so-called α4/α5/α6 triangle of PP1, which is close to the catalytic site (*11*). In contrast, I3 is a small, heat-stable inhibitor which contains a degenerate, so-called RVxF motif that is present in a majority of PP1 interactors and binds to a hydrophobic channel of PP1 that is remote from the catalytic site (*1*, *12*). The RVxF motif functions as an anchor for PP1 and thereby enables the interaction of secondary, lower-affinity binding sites that control the activity and substrate specificity of PP1 (*13*).

Since Sds22 and I3 interact with different sites of PP1, it is possible that they can interact simultaneously and form a heterotrimeric complex. We have recently found that Sds22 and Ypi1 indeed form a heterotrimeric complex with Glc7, the budding yeast orthologue of PP1 (*9*). Here, we report the characterization of a similar, but not identical, complex in mammals and show that Sds22 has the ability to convert PP1 into an inactive conformation.

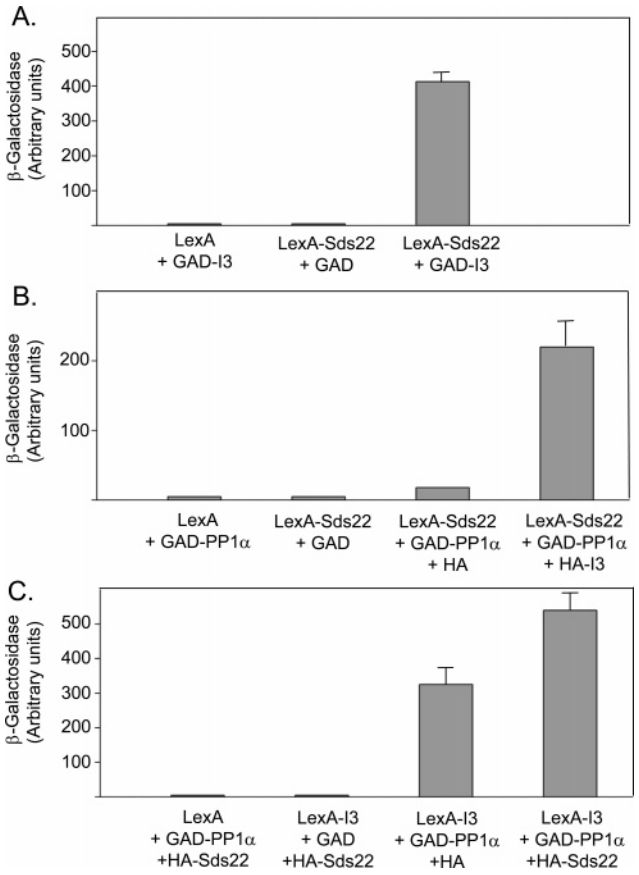

FIGURE 1: Two-hybrid interactions among Sds22, PP1, and I3. (A) TAT7 yeast cells were transformed with pACT2, pACT2-I3, pBTM116, and/or pBTM-Sds22, encoding GAD, GAD-I3, LexA, and LexA-Sds22, respectively. Transformants were grown in selective SC medium with 2% glucose until an OD_{600} of 0.5 was reached. The interaction between the expressed proteins was derived from the assay of β-galactosidase activities. The values represent means ± the standard error ($n = 4-6$). (B) TAT7 cells containing plasmid pBTM116 or pBTM-Sds22 were transformed with pACT2, pACT2-PP1α, pWS93, and/or pWS-I3, encoding GAD, GAD-PP1α, HA, and HA-I3, respectively. Transformants were analyzed as described above. (C) TAT7 cells containing plasmid pBTM116 or pBTM-I3 were transformed with pACT2, pACT-PP1α, pWS93, and/or pWS-Sds22. The latter plasmid encodes HA-Sds22. Transformants were analyzed as indicated for panel A. The expression of all constructs was verified by immunoblotting (not illustrated).

EXPERIMENTAL PROCEDURES

Plasmids. Full-length human I3 and I3-(84−125) were introduced between the *Xho*I and *Xma*I sites of pEGFP-C1 (Clontech) and between the *Eco*RI and *Bam*HI sites of RFP-C1, yielding expression vectors for EGFP-I3, EGFP-I3-(84−125), and RFP-I3. I3 was also introduced between the *Eco*RI and *Sal*I sites of the pWS93 and pBTM116 yeast expression vectors (*7*) to generate HA−I3 and LexA−I3 fusion proteins, respectively. A *Bam*HI−*Sal*I fragment from pBTM-I3 was subcloned into plasmid pACT2 (*7*) to generate a GAD−I3 fusion protein. NIPP1-(143−224), human I3, and human Sds22 were also subcloned in the pGMEX-T1 vector (Amrad

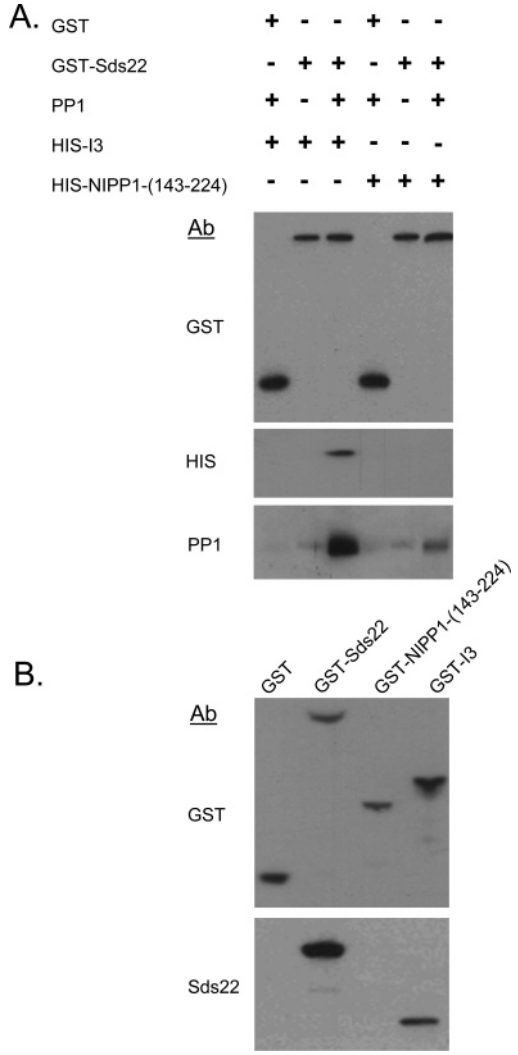

FIGURE 2: GST pulldown experiments confirm the interaction among Sds22, PP1, and I3. (A) Purified GST-tagged Sds22 (240 nM) was incubated for 60 min at 10 °C with the same concentration of either purified His-I3 or His-NIPP1-(143−224), in the absence or presence of 200 nM purified PP1. Following the pulldown of the GST fusion with glutathione agarose, the washed beads were screened for the presence of GST−Sds22, His-tagged proteins, and PP1 by immunoblotting. (B) COS1 cells were transfected with GST, GST−Sds22, GST−NIPP1-(143−224), or GST−I3. The GST fusions were pulled down with glutathione agarose, and the pellets were analyzed for the presence of GST and Sds22 by immunoblotting.

Pharmacia Biotech), downstream of the glutathione *S*-transferase (GST) encoding cassette. In this vector, the *Bam*HI−*Xma*I sites were used for the cloning of Sds22 and I3 and the *Xma*I−*Not*I sites for NIPP1-(143−224). Sds22 was further subcloned in the *Eco*RI and *Bam*HI sites of pEGFP-C1 vector and in the *Bam*HI site of the pSG5 vector (Stratagene), with a triple FLAG-tag cassette inserted in its *Eco*RI site and between the *Eco*RI and *Sal*I sites of the pWS93, pWS-GST, and pBTM116 yeast expression vectors (*7*) to generate HA−Sds22, GST−Sds22, and LexA−Sds22 fusion proteins. A *Bam*HI−*Sal*I fragment from pBTM-Sds22 was subcloned into plasmid pACT2 (*7*) to generate a GAD−Sds22 fusion protein. I3 was subcloned with the *Xho*I−*Bam*HI fragment into the pET-16b vector (Novagen) for expression in bacteria as a polyhistidine-tagged protein. All the indicated mutants of the Flag−Sds22 and EGFP−I3 fusion proteins were made according to the QuikChange protocol (Stratagene), with the appropriate primers and templates. To generate EGFP−I3-(1−54), EGFP−I3-(1−84), and FLAG−Sds22-(1−332), stop codons were introduced into codons 55 and 85 of EGFP−I3 and codon 333 of FLAG−Sds22. All constructs and mutants were verified by DNA sequencing.

Antibodies, Recombinant Proteins, and Peptides. Polyhistidine-tagged I3 and NIPP1-(143−224) were expressed in bacteria and purified on Ni^{2+}-Sepharose, as described previously (*14*). GST-tagged human Sds22 was expressed in yeast and purified as described previously (*9*). Human recombinant polyhistidine-tagged I3 was used to raise antibodies in rabbits. The anti-I3 antibodies were affinity-purified on His-I3 linked to CNBr-activated Sepharose 4B (GE Healthcare). A monoclonal anti-FLAG antibody (Stratagene), polyclonal anti-GST (Santa Cruz Biotechnology), and anti-HIS antibodies (Qiagen) were purchased. The digoxygenin-labeled anti-Sds22 antibody was prepared as described previously (*15*), using the digoxygenin protein labeling kit from Roche Molecular Biochemicals. Anti-digoxygenin antibodies linked to alkaline phosphatase were delivered by Roche Applied Science. Monoclonal anti-PP1 antibodies were purified on protein A-Sepharose CL-4B (GE Healthcare). The hybridoma clone producing these antibodies was a gift from J. Vandenheede (University of Leuven). Peptides were synthesized on a Milligen 9050 instrument, using the *N*-(9-fluorenyl)methoxycarbonyl method.

Preparation of Phosphosubstrates and Assays. The phosphosubstrates glycogen phosphorylase *a*, casein, myelin basic protein, and histone 2A were prepared as described previously (*16*). GST-tagged human Sds22, expressed in yeast, bacterially expressed His-tagged I3, or the indicated synthetic peptides were assayed as inhibitors of PP1. Protein phosphatase activities were determined at 30 °C from the rate of dephosphorylation of the substrates. The extent of dephosphorylation was assessed from the released acid-soluble radioactivity. The phosphorylase phosphatase activity was assayed either as such ("spontaneous" activity) or after preincubation with trypsin (0.1 mg/mL) for 5 min at 30 °C ("trypsin-revealed" activity). The action of trypsin was arrested by the addition of soybean trypsin inhibitor (1 mg/mL, Sigma). Prior to the addition of the phosphosubstrate, the putative inhibitory proteins or fragments were preincubated with PP1 for the indicated periods of time.

Cell Cultures, Immunoprecipitations, GST Pulldowns, and Gel Filtration. COS1 cells were grown in Dulbecco's modified Eagle's medium with 10% fetal calf serum. Transfection with the indicated plasmids was carried out using polyethylenimine (PEI) obtained from Sigma-Aldrich. Cell transfection experiments with PEI were performed in DMEM with 5% fetal calf serum. One day after transfection, the medium was replaced with fresh DMEM, supplemented with 10% fetal calf serum. Forty-eight hours after transfection, the cells were washed twice with PBS [1.8 mM KH_2PO_4, 8.1 mM Na_2HPO_4, and 150 mM NaCl (pH 7.4)] and harvested in a lysis buffer containing 50 mM Tris-HCl (pH 7.4), 0.3 M NaCl, 0.5% Triton X-100, 0.5 mM phenylmethanesulfonyl fluoride, 1 mM dithiothreitol, 0.5 mM benzamidine, and 5 μM leupeptin. Following centrifugation (10 min at 6000*g*), the supernatants (cell lysates) were used either for the immunoprecipitation with anti-EGFP, anti-Flag, or anti-I3 antibodies and protein A-TSK-Sepharose (Affiland)

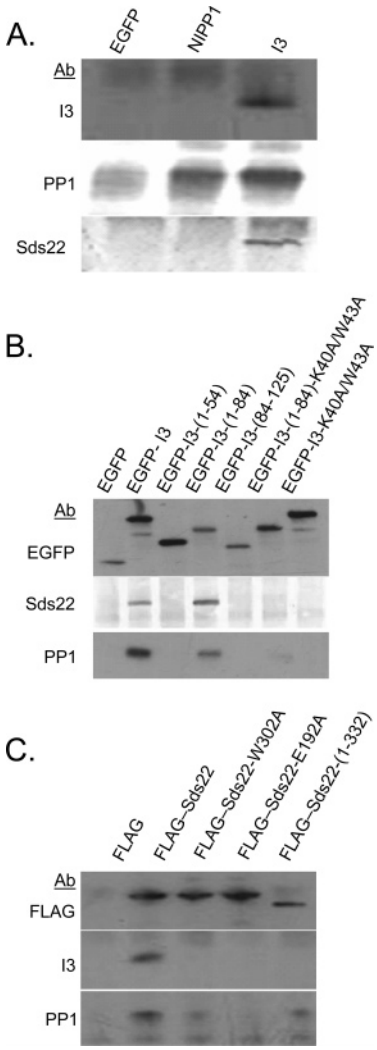

FIGURE 3: Sds22 interacts with I3 via PP1. (A) COS1 cell lysates were used for the immunoprecipitation of endogenous NIPP1 or I3. EGFP antibody was added under the control condition. The immunoprecipitates were examined for the presence of PP1 and Sds22 by immunoblotting. (B) COS1 cells were transfected with indicated EGFP fusions of I3 or EGFP alone. The EGFP−I3 fusions were immunoprecipitated, and the pellets were analyzed by immunoblotting with anti-EGFP, anti-Sds22, and anti-PP1 antibodies. (C) Flag fusions of the indicated Sds22 (mutants) or the Flag tag alone were expressed in COS1 cells. Subsequently, the Flag fusions were immunoprecipitated from the cell lysates and the immunoprecipitates were used for Western blotting using anti-FLAG, anti-I3, and anti-PP1 antibodies.

or for the pulldown of GST constructs with glutathione agarose (Sigma). Before being immunoblotted, the precipitates were washed once with PBS containing 0.1% NP40 and 0.1 M LiCl and twice with PBS with 0.1% NP40. Finally, the precipitates were analyzed by immunoblotting or assayed with glycogen phosphorylase *a* as substrate (*16*).

A HeLa cell lysate was applied to a Superdex-200 gel filtration column (24 mL) (Amersham Pharmacia Biotech), equilibrated with TBS. Fractions of 0.25 mL were collected and assayed for immunodetectable Sds22, I3, and PP1.

Confocal Microscopy. Confocal images were obtained with a Zeiss (Jena, Germany) LSM-510 laser-scanning confocal microscope equipped with the Zeiss Axiovert 100 M (Plan Apochromat 40 × 1.30 NA oil immersion objective). For the simultaneous imaging of EGFP and RFP fluorescence, both labels were excited in different tracks with the 488 nm line of an argon laser and the 543 nm line of a helium−neon laser, respectively. The emission from each fluorochrome was detected using 505−530 nm (fluorescein thiocyanate) and 560−615 nm (TRITC) band-pass filters.

RESULTS

Characterization of a Heterotrimeric Complex of Sds22, PP1, and Inhibitor-3. To test whether human Inhibitor-3 (I3) and Sds22, like their yeast orthologues, interact with each other as well as with PP1, we first performed yeast two-hybrid assays. For this purpose, we prepared a GAD−I3 fusion protein containing the activating domain of the Gal4 transcription factor and a LexA−Sds22 fusion protein, containing the DNA-binding domain of the bacterial LexA transcription factor. As shown in Figure 1A, GAD−I3 and LexA−Sds22 proteins did indeed interact strongly in two-hybrid assays, and this interaction was not mediated by the GAD and LexA tags (Figure 1A). The LexA−Sds22 protein also interacted with the GAD−PP1α fusion protein, and interestingly, the strength of this interaction was increased ∼15-fold by the coexpression of HA−I3 (Figure 1B). Likewise, the strength of the interaction between LexA−I3 and GAD−PP1α was increased by some 50% following the coexpression of HA−Sds22 (Figure 1C). Thus, these two-hybrid data revealed that the strength of the interaction between PP1 and either Sds22 or I3 was increased by the overexpression of I3 or Sds22, respectively. We have recently reported similar results with the corresponding yeast orthologues Sds22, Glc7, and Ypi1 (*9*), suggesting that the most stable complex comprises all three components.

To explore the interaction among Sds22, I3, and PP1 in further detail, we performed reconstitution experiments with the purified recombinant components. Interestingly, pulldown experiments with GST−Sds22 showed only cosedimentation with His-tagged I3 when PP1 was added to the mixture, indicating that the interaction between Sds22 and I3 is mediated by PP1 (Figure 2A). Since the RVxF-binding channel of Sds22-associated PP1 is expected to be accessible (*11*), one could envisage that any PP1 interactor with an RVxF motif could be retained by the Sds22−PP1 complex. To test this possibility, we examined the ability of the Sds22−PP1 complex to bind His-tagged NIPP1-(143−224), which is structurally unrelated to I3 but is similar in size and also has a functional RVxF motif. However, NIPP1-(143−224) could not be pulled down with GST−Sds22, in the absence or presence of PP1, reinforcing the specificity of the interaction between the Sds22−PP1 complex and I3. The weaker binding of PP1 to GST−Sds22 in the presence of His-NIPP1-(143−224) can be readily explained by competition between GST−Sds22 and NIPP1-(143−224) for the binding of PP1. To further examine whether other RVxF interactors can form a complex with Sds22−PP1, we performed pulldown experiments in cell lysates from COS1 cells that overexpressed GST−Sds22, GST−NIPP1-(143−224), or GST−I3. Figure 2B shows that GST−Sds22 and endogenous Sds22 were present in pulldowns of GST−Sds22 and GST−I3, respectively. However, Sds22 could not be detected in pulldowns of GST−NIPP1-(143−224), confirming the specificity of the interaction of I3 with the Sds22 complex.

We have subsequently explored the interaction among endogenous I3, Sds22, and PP1 in COS1 cell lysates, using

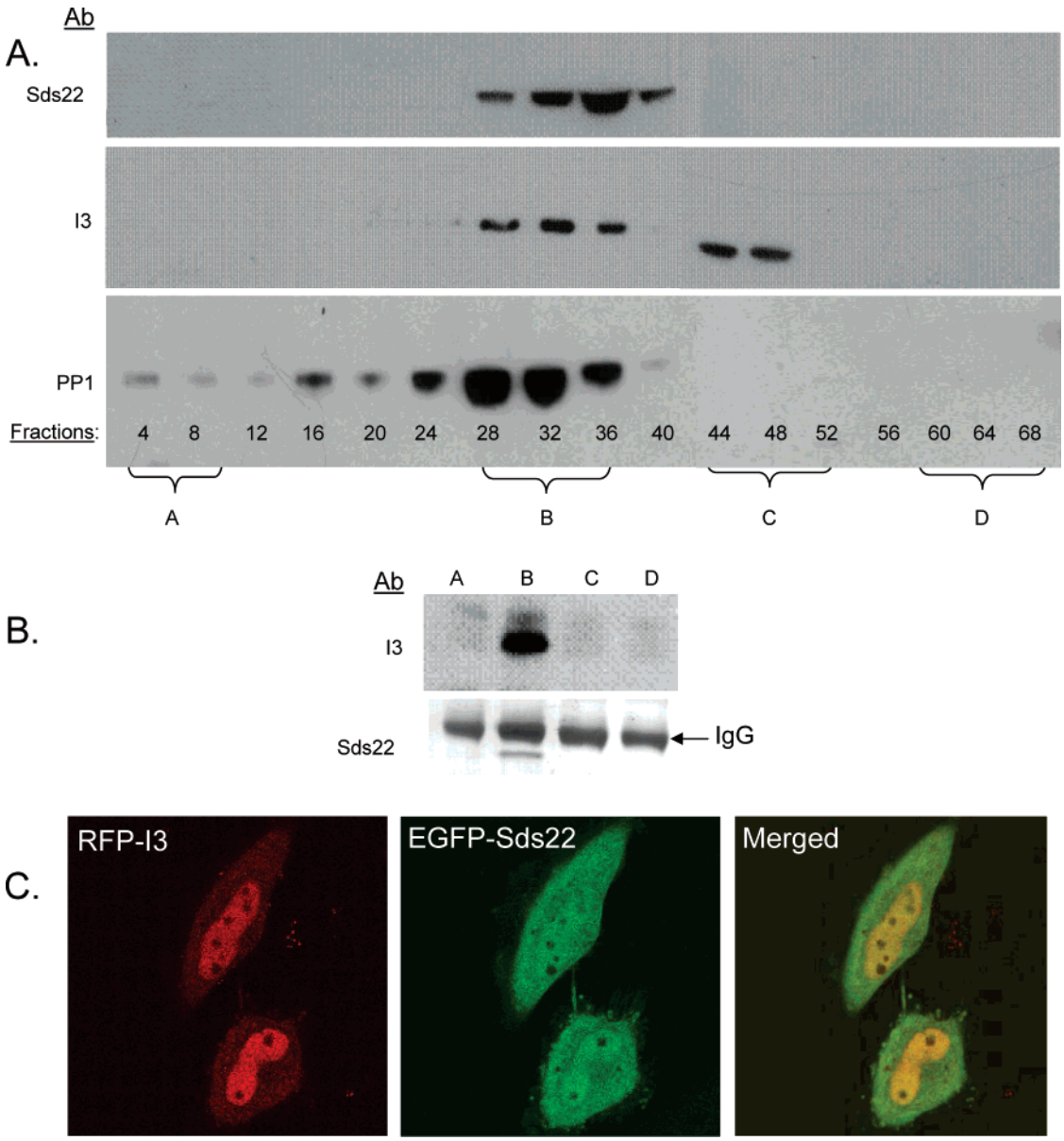

FIGURE 4: Sds22 and I3 comigrate during gel filtration and colocalize in intact cells. (A) Extracts from HeLa cells were loaded on a FPLC Superdex 200 gel filtration column. Aliquots were analyzed by SDS−PAGE and immunodetected with either Sds22, I3, or PP1 antibodies. (B) Four pools of eight fractions (1−8, 28−36, 44−52, and 60−68) were used for immunoprecipitation of endogenous I3. The immunoprecipitates were examined for the presence of I3 and Sds22 by immunoblotting. (C) Localization of EGFP−Sds22 and RFP−I3 in transiently transfected HeLa cells. The middle panel shows the localization of EGFP−Sds22 in live HeLa cells, with the RFP-I3 image in the left panel and the two images merged in the right panel.

anti-I3 antibodies. The immunoprecipitation of endogenous I3 resulted in the coprecipitation of both PP1 and Sds22 (Figure 3A). In contrast, immunoprecipitates of endogenous NIPP1 contained PP1 but no Sds22. Finally, neither I3, PP1, nor Sds22 was immunoprecipitated with a control antibody (anti-EGFP).

To further map the sites of interaction of Sds22, I3, and PP1, we studied their interaction in cell lysates prepared from COS1 cells that overexpressed Flag-tagged Sds22 (mutants), EGFP-tagged I3 (mutants), or the tags alone. As observed for endogenous I3 (Figure 3A), EGFP-tagged I3 interacted with both endogenous Sds22 and PP1 in immunoprecipitation experiments (Figure 3B). EGFP-I3-(1−84), which comprises the N-terminal two-thirds of I3, also bound to both Sds22 and PP1. Importantly, mutation of the PP1-binding RVxF motif of I3, as in EGFP−I3-K40A/W43A or EGFP−I3-(1−84)-K40A/W43A, abolished the binding to both Sds22 and PP1, confirming that the I3−Sds22 interaction is mediated by PP1. Sds22 and PP1 did not co-immunoprecipitate with EGFP, EGFP−I3-(84−125), or EGFP−I3-(1−54). The lack of co-immunoprecipitation of EGFP−I3-(1−54) and PP1 was unexpected since this I3 fragment harbors the RVxF motif. Since PP1 did, however, interact with EGFP−I3-(1−84), these data suggest that the high-affinity binding of I3 to PP1 requires, in addition to the RVxF motif, residues 54−83 of I3.

Endogenous PP1 and I3 co-immunoprecipitated with Flag-Sds22, but not with the Flag tag alone (Figure 3C). However, neither PP1 nor I3 co-immunoprecipitated with Flag-Sds22 that was mutated (W302A or E192A) in its previously established PP1-binding site (*11*), consistent with the notion that the binding of I3 is mediated by PP1. Finally, the binding of PP1 and I3 was also abolished by deletion of the C-terminus of Sds22. This deletion is expected to cause major

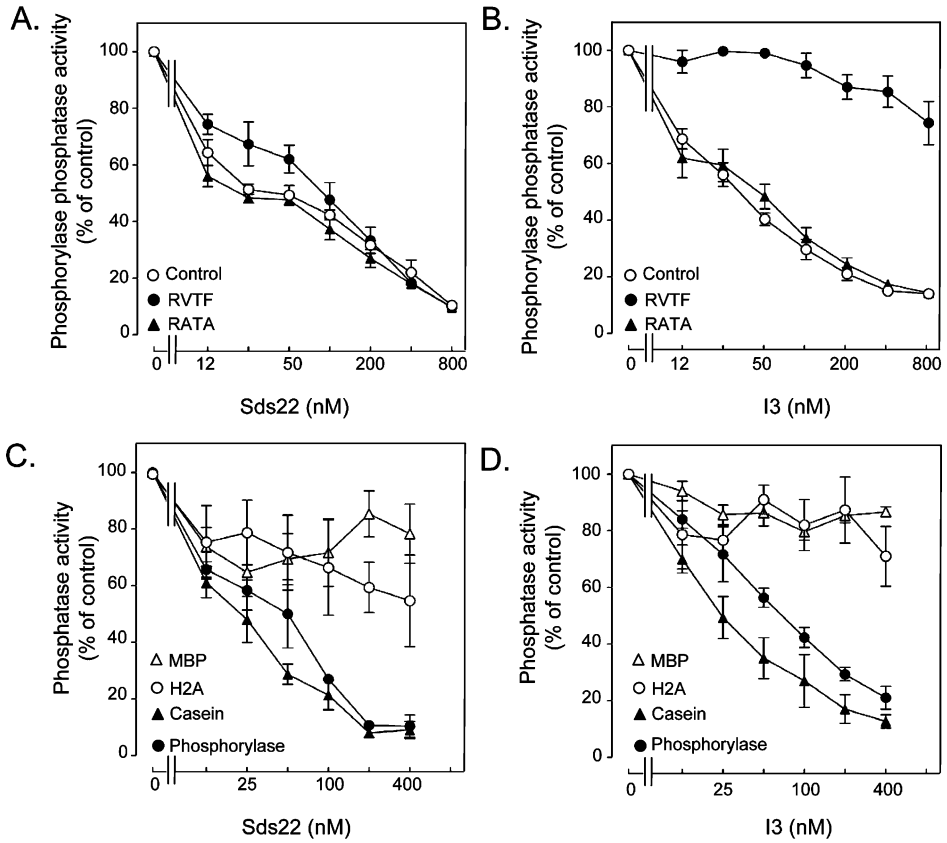

FIGURE 5: Sds22 and I3 are substrate-dependent inhibitors of PP1. (A) The phosphorylase phosphatase activity of 1 nM PP1 was measured with the indicated concentrations of Sds22, as such (control) or after the addition of 80 μM NIPP1-(197−206) (RVTF) or NIPP1-(197−206)-V201A/F203A (RATA) decapeptides. (B) Like panel A but with I3 as an inhibitor. (C) Effect of the indicated concentrations of Sds22 on the activity of PP1, using myelin basic protein (MBP), histone H2A, casein, or phosphorylase *a* as a substrate. (D) Like panel C but with I3 as an inhibitor. The results represent means ± the standard error ($n = 3$).

conformational changes since the deleted fragment corresponds to the LRR cap structure, necessary for the shielding of the hydrophobic core of Sds22 from solvent (*17*).

Finally, to examine whether a free pool of Sds22 or I3 also exists, we performed gel filtration with a HeLa cell lysate on Sephadex G200 (Figure 4A). Immunoblot analysis revealed that Sds22, I3, and a considerable fraction of PP1 comigrated during gel filtration. An additional band was detected with the anti-I3 antibodies in later fractions. However, the latter band migrated with a size smaller than that expected from I3 and is therefore likely to represent a degradation product or a nonspecific interaction. We have also confirmed the Sds22−I3 interaction following gel filtration by co-immunoprecipitation of Sds22 and I3 (Figure 4B).

We have also explored the subcellular distribution of the Sds22−I3 complex (Figure 4C). Since the available antibodies were not suited for immunohistochemistry, we have performed live imaging of HeLa cells following the transient expression of RFP-tagged I3 and EGFP-tagged Sds22. The data show that RFP−I3 is enriched in the nucleus and that EGFP−Sds22 is both nuclear and cytoplasmic. Thus, I3 and Sds22 colocalize mostly in the nucleus.

Sds22 and I3 Are Substrate-Dependent Inhibitors of PP1. I3 (*12*) and a fragment of Sds22 (*18*) were previously demonstrated to inhibit PP1. Here we show that human GST-tagged Sds22, expressed in yeast and affinity-purified on gluthatione agarose, inhibited the phosphorylase phosphatase activity of PP1 with an IC_{50} of ∼50 nM (Figure 5A). I3 inhibited PP1 with a similar potency (Figure 5B). However, the combination of Sds22 and I3 did not increase their inhibitory concentration (not illustrated), showing that these inhibitors do not act synergistically. The inhibition of PP1 by I3 was alleviated by competition with the synthetic decapeptide NIPP1-(197−206), containing the RVxF motif of NIPP1 (RVTF peptide, Figure 5B). No competition was obtained when the Val and Phe of the RVxF motif in this decapeptide were replaced with an Ala (RATA peptide). The inhibition of PP1 by Sds22 was not affected by the addition of either the RVTF or RATA peptide (Figure 5A), consistent with the notion that Sds22 does not bind to PP1 via an RVxF motif (*11*).

Some interactors of PP1 function as substrate specifiers, implying that their effect on PP1 varies with the substrate used (*1*). To examine whether this also applies to Sds22 and I3, we compared their inhibitory potency using glycogen phosphorylase, casein, myelin basic protein, and histone H2A as substrates of purified PP1. Both Sds22 and I3 inhibited the dephosphorylation of glycogen phosphorylase and casein with an IC_{50} of 25−100 nM, but they did not have major effects on the dephosphorylation of myelin basic protein and histone H2A by PP1 (Figure 5C,D). These data clearly show that the inhibition of PP1 by Sds22 and I3 is substrate-dependent.

Sds22 largely consists of 11 LRRs, and these mediate the interaction with PP1 (*12*). We have examined whether the inhibition of PP1 by Sds22 could be reproduced by one or several of its 11 LLRs. We found that only two of the

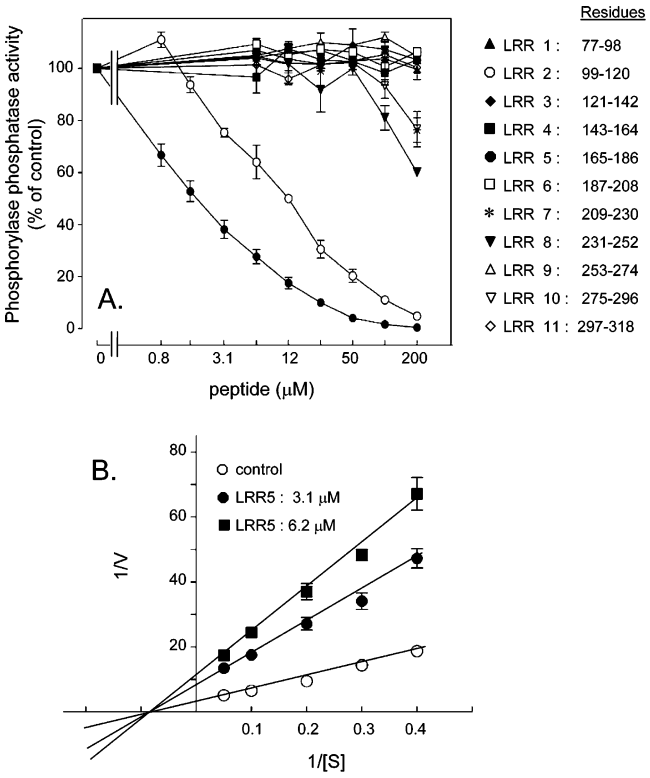

FIGURE 6: Inhibition of PP1 by the synthetic LLRs of Sds22. (A) The phosphorylase phosphatase activity of 1 nM PP1 was measured in the presence of the indicated concentrations of each of the 11 synthetic LRRs of Sds22. The results represent means ± the standard error ($n = 3$). (B) PP1 was assayed as such (control) or in the presence of the indicated concentrations of LLR5 at various concentrations of the substrate phosphorylase *a*. Shown is a Lineweaver−Burk plot with means ± the standard error of three experiments. The lines show the best fit computed by linear regression analysis. The results represent means ± the standard error ($n = 3$).

synthetic LRRs, i.e., repeats 2 and 5, inhibited the phosphorylase phosphatase activity of PP1 with IC_{50} values of ∼10 and ∼2 μM, respectively (Figure 6A). Lineweaver−Burk plots identified the LRR5 peptide as a noncompetitive inhibitor (Figure 6B).

Sds22 Slowly Converts PP1 into an Inactive Conformation. It is well-established that the PP1 interactor Inhibitor-2 (I2) not only instantaneously inhibits the activity of PP1 but also slowly converts PP1 into an inactive conformation (*19*). The "inhibition" of PP1 by I2 can be reversed by trypsinolysis, which destroys I2 and hydrolyzes the C-terminus of PP1, thereby releasing the fully active catalytic core of PP1 (Figure 7A). In contrast, the "inactivation" of PP1 cannot be reversed by proteolysis since inactivated PP1 is destroyed by trypsin. We have found that purified Sds22 also converts PP1 into a trypsin-sensitive conformation in a time-dependent manner, as evidenced by the gradual loss of the trypsin-revealed phosphorylase phosphatase activity [Figure 7B (●)]. An activity loss by 50% was obtained within 10−15 min at 30 °C. I3 had an only moderate inactivating effect (▲) and the Sds22-induced inactivation was not affected by the addition of I3 (△). However, the inactivation of PP1 by Sds22 did reduce the affinity of the complex for I3, as indicated by the reduced level of sedimentation (ca. 80%) of I3 by the inactive complex of GST−Sd22 and PP1 (not illustrated). Figure 7C confirmed by immunoblotting that PP1 that had been preincubated with Sds22 was indeed destroyed by trypsin. We have also examined whether any of the synthetic LRRs of Sds22 could inactivate PP1. While most LRRs had a slight inactivating effect, LRR5, which is also the most inhibitory LRR of Sds22 (Figure 5A), was by far the best PP1 inactivator (Figure 6D). LRR5 caused a 50% inactivation in 60 min.

Using mass spectrometry analysis, we identified Lys26 and Arg74 as the major sites of trypsinolysis in Sds22-inactivated PP1 (not illustrated). Sds22 was mainly proteolyzed in this experiment after Lys134, Lys179, Lys223, and Arg341. I3, on the other hand, did not affect the sensitivity of the catalytic core of PP1 to trypsin.

The inactivation of PP1 by I2 is realized at concentrations of I2 much lower than those that are required for the inhibition of PP1 (*19*). Figure 8 shows that this also applies to Sds22. Indeed, the IC_{50} for the trypsin-revealed inactivation of PP1 amounted to ∼10 nM Sds22, which is at least 1 order of magnitude lower than that required for the inhibition of PP1. These data suggest that the inactivation and inhibition of PP1 by Sds22 are distinct phenonema and stem from the interaction of Sds22 with high-affinity and low-affinity binding sites, respectively. The different concentrations of Sds22 needed to inhibit and inactivate PP1 also enabled us to examine whether the Sds22-induced inactivation is substrate-dependent. Incubation of PP1 with a concentration of Sds22 (8 nM) that was not inhibitory (see Figure 8) resulted after 60 min at 30 °C in a loss of the PP1 activity of ∼50%, as measured with phosphorylase (not illustrated). The same inactivation was obtained using casein, myelin basic protein, and histone H2A as substrates. The latter activities were measured without prior trypsinolysis and can thus not be ascribed to proteolysis of PP1, clearly showing that the Sds22-induced conformational change in PP1 represents an inactivation. A similar incubation without Sds22 did not measurably affect these activities of PP1. Thus, the Sds22-induced inactivation of PP1, in contrast to its inhibition of PP1 (Figure 5C), is substrate-independent.

The inactivation of PP1 by I2 can be reversed by trypsinolysis in the presence of Mn^{2+} or by the transient phosphorylation of I2 with protein kinase GSK3 (*19*). However, these treatments did not reactivate Sds22-inactivated PP1 (not shown), and Sds22-inactivated PP1 could not be reactivated by addition of an excess of I2 in the presence of GSK3 and MgATP. We have previously established experimental conditions, i.e., an incubation at pH 8 or with either 150 mM KCl or 0.3 mM NaF, that hamper the I2-mediated inactivation of PP1 (*20*). Of these conditions, only the addition of KCl also prevented the time-dependent inactivation of PP1 by Sds22 (Figure 9A and data not shown) and by the synthetic LRR5 peptide of Sds22 (not illustrated). Consistent with these findings, KCl also inhibited the Sds22-mediated sensitization of PP1 to trypsinolysis (Figure 9B).

We have subsequently used the anti-inactivation effect of KCl to examine whether the Sds22−PP1−I3 complex is inactive in vivo or wether the inactivation occurs gradually after cell fractionation, as appears to be the case for the I2-induced inactivation (*20*). For this purpose, we used cell lysates that were freshly prepared from COS1 cells in the presence of 300 mM KCl. Immunoprecipitates of endogenous I3 and NIPP1 from these lysates contained similar amounts

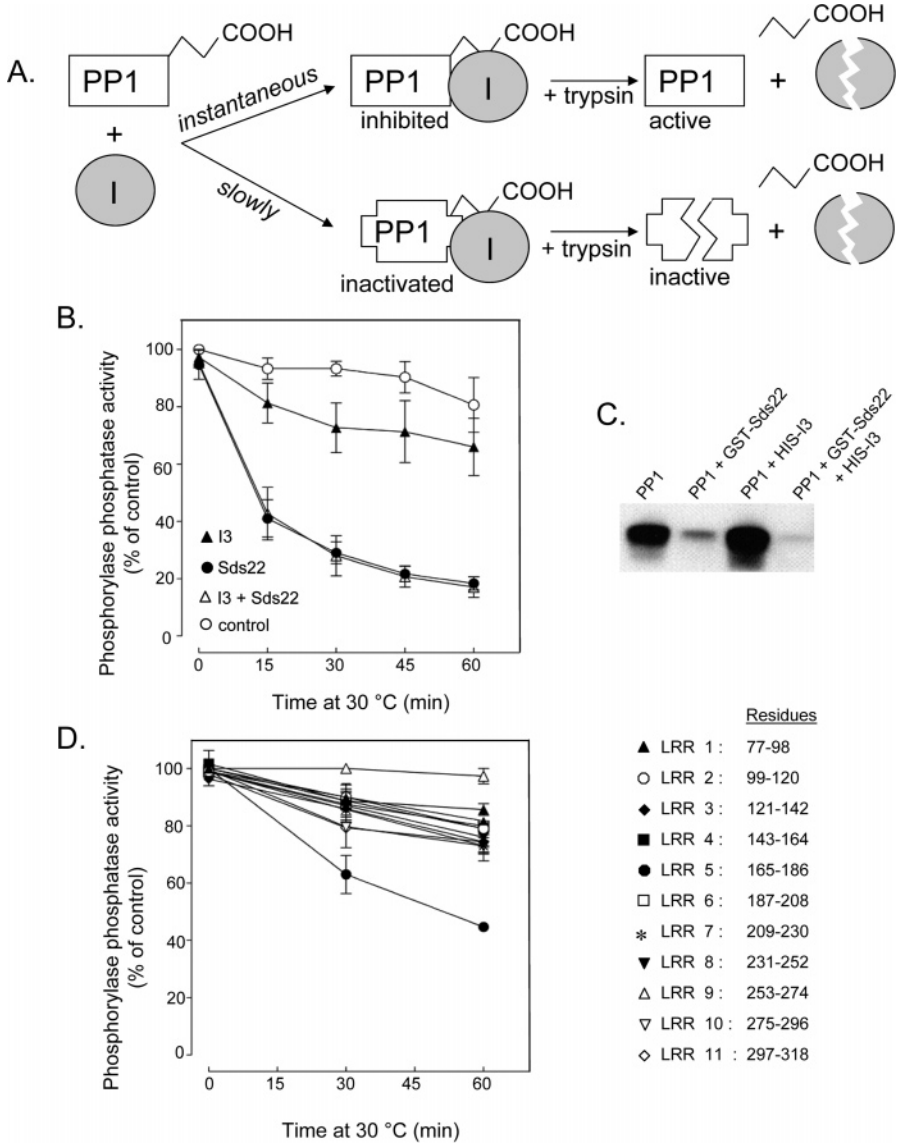

FIGURE 7: Sds22 slowly converts PP1 into a trypsin-sensitive conformation. (A) Scheme illustrating the difference between inhibition and inactivation of PP1. The inhibition is reversed by trypsinolysis of the inhibitor (I). Trypsin also hydrolyzes the C-terminus of PP1, yielding a fully active phosphatase. Inactivated PP1 is completely destroyed by trypsin. (B) PP1 (2 nM) was incubated at 30 °C as such (○), in the presence of either 78 nM GST−Sds22 (●) or 30 nM His-I3 (▲), or in the presence of both GST−Sds22 and His-I3 (△). At the indicated time points, aliquots were assayed for trypsin-revealed phosphorylase phosphatase activity. The results represent means ± the standard error ($n = 3$). (C) PP1 was incubated for 60 min at 30 °C in the absence or presence of GST−Sds22 and/or His-I3. Subsequently, an aliquot was subjected to trypsinolysis and the trypsin-resistant core of PP1 was quantified by immunoblotting with an anti-PP1 antibody. (D) Time-dependent effect of the synthetic LRRs of Sds22 (16 μM) on the trypsin-revealed phosphorylase phosphatase activity of PP1 (2 nM).

of PP1, as determined by immunoblotting (Figure 10A). However, the trypsin-revealed phosphorylase phosphatase activity associated with I3-associated PP1 was ∼5−10 fold lower than that associated with NIPP1 (Figure 10B). Similarly, pulldowns of GST−Sds22, GST−NIPP1-(143−224), or GST−I3 from COS1 cells that overexpressed these fusions all resulted in the coprecipitation of immunodetectable PP1 (Figure 10C). However, in spite of the fact that much less PP1 was coprecipitated with GST−NIPP1-(143−224) than with GST−Sds22 or GST−I3, the trypsin-revealed phosphorylase phosphatase activity that was associated with GST−NIPP1-(143−225) was many-fold higher (Figure 10D). Collectively, these data indicate that PP1 is largely present in an inactive conformation in the Sds22−PP1−I3 complex in vivo.

DISCUSSION

A Novel PP1 Holoenzyme Containing Sds22 and I3. An emerging theme in the PP1 field is that the catalytic subunit forms complexes with two regulatory proteins, one of which functions as an inhibitor or chaperone of PP1. The best characterized holoenzymes of this nature are PP1 complexed to (1) Inhibitor-1 and the growth arrest and DNA damage-inducible protein GADD34 (*21*), (2) Inhibitor-2 and protein kinase NEK2 (*22*), and (3) CPI17 and the myosin targeting subunit MYPT1 (*23*). We describe here a novel mammalian heterotrimeric PP1 holoenzyme that contains the ancient PP1 interactors Sds22 and I3. This complex resembles the MYPT−PP1−CPI17 holoenzyme in that it also contains two interactors with distinct PP1-binding motifs. From another perspective, the Sds22−PP1−I3 complex resembles the

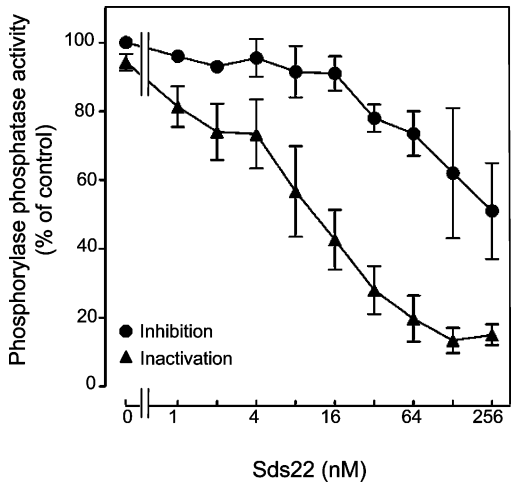

FIGURE 8: Inhibition and inactivation of PP1 occur at different concentrations of Sds22. The figure shows the effect of the indicated concentrations of GST−Sds22 on the spontaneous and trypsin-revealed phosphorylase phosphatase activity of 6 nM PP1. The trypsin-revealed activity was assayed after a preincubation of PP1 with Sds22 for 60 min at 30 °C. The results represent means ± the standard error ($n = 3$).

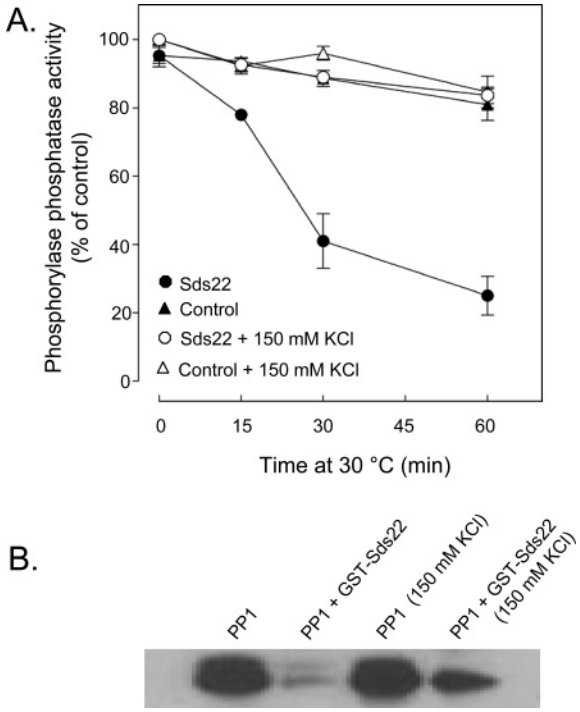

FIGURE 9: KCl prevents the Sds22-mediated inactivation of PP1. (A) PP1 (2 nM) was incubated at 30 °C in the absence or presence of GST−Sds22 (78 nM), with or withour 150 mM KCl, as indicated. At the indicated time points, aliquots were assayed for trypsin-revealed phosphorylase phosphatase activities. The results represent means ± the standard error ($n = 3$). (B) Aliquots of the samples at 60 min were also analyzed by immunoblotting with an anti-PP1 antibody.

NEK2−PP1−I2 complex in that they both contain a protein, i.e., Sds22 or I2, which slowly converts PP1 into an inactive, trypsin-sensitive conformation, yet the conformational changes induced by Sds22 and I2 appear to be different since only the I2-mediated inactivation is blocked by an alkaline pH and by NaF and is reversed by trypsinolysis in the presence of Mn^{2+} (*20*).

We have studied the Sds22−PP1−I3 complex using a combination of different techniques such as yeast two-hybrid analysis, GST pulldown experiments with purified components, reciprocal immunoprecipations from cell lysates, subcellular localization studies, and gel filtration analysis. Our data show that PP1 is sandwiched between Sds22 and I3. Indeed, purified Sds22 and I3 formed a complex only when PP1 was added (Figure 2A), and mutation of the PP1-binding sites of either Sds22 or I3 abolished the formation of the heterotrimeric complex (Figure 3B,C). This differs from the corresponding complex in yeast where mutation of the PP1-binding site of Ypi1 did not hamper the interaction with Sds22 (*9*).

While our data strongly suggest that PP1 mediates the interaction between Sds22 and I3, we cannot rule out the possibility that Sds22 also interacts directly with I3 once both proteins are recruited to their high-affinity binding sites on PP1. Such secondary interactions could explain why I3 cannot be replaced by another PP1 interactor, such as NIPP1-(143−224), with a similar size and PP1-binding motif (Figure 2A,B). In any case, the latter finding demonstrates that the interaction of I3 with the Sds22−PP1 complex is specific. Finally, confocal microscopy revealed at least a partial colocalization EGFP−Sds22 and RFP−I3 in HeLa cells (Figure 4C).

Inhibition versus Inactivation of PP1. Both Sds22 and I3 instantaneously inhibit the activity of PP1 toward selected substrates (Figure 5C,D). This is consistent with previous findings that Sds22-associated PP1 can dephosphorylate histones but not glycogen phosphorylase (*24*). These data suggest that Sds22 and I3 may not be true PP1 inhibitors but rather function as substrate specifiers, as is the case for numerous PP1-interacting proteins (*1*, *2*). The inhibition of PP1 by Sds22 could be reproduced with synthetic LRR2 and LRR5 (Figure 6), in agreement with previous data implicating the LRRs of Sds22 in its interaction with PP1 (*11*, *18*, *24*). Unexpectedly, Sds22 also slowly converted PP1 into an inactive, trypsin-sensitive conformation (Figure 7), and this inactivation occurred at concentrations of Sds22 much lower than those required for the inhibition of PP1 (Figure 8). This could imply that the Sds22-mediated inactivation of PP1 may be physiologically more relevant than its inhibition by Sds22. Importantly, an inactive complex of Sds22, PP1, and I3 could also be identified in cell lysates (Figure 10), even when the lysates were freshly prepared in the presence of KCl, which blocks the Sds22-mediated inactivation (Figure 9). This is clear evidence that the inactive complex also exists in vivo and implies that previous estimates of the spontaneous and trypsin-revealed Sds22-associated PP1 activity grossly underestimate the amount of PP1 that is present in the complex (*19*).

Possible Functions of the Sds22−PP1−I3 Complex. Our finding that Sds22, PP1, and I3 are present in the cell as a catalytically inactive complex is not in contrast with the recent proposal that Sds22 functions as a chaperone and a positive regulator of PP1 (*8*, *10*). Sds22 possibly plays a role in the regulation of PP1 activity, for example, by converting newly synthetized PP1 into an active conformation and/or delivering it to specific targeting subunits. This hypothesis implies that a mechanism for activating Sds22-associated PP1 must exist. By analogy with the mechanism of activation of I2-associated PP1, we speculate that the activation of Sds22- and I3-associated PP1 is regulated by the phosphorylation of Sds22 and/or I3. As far as I3 is concerned, at present we

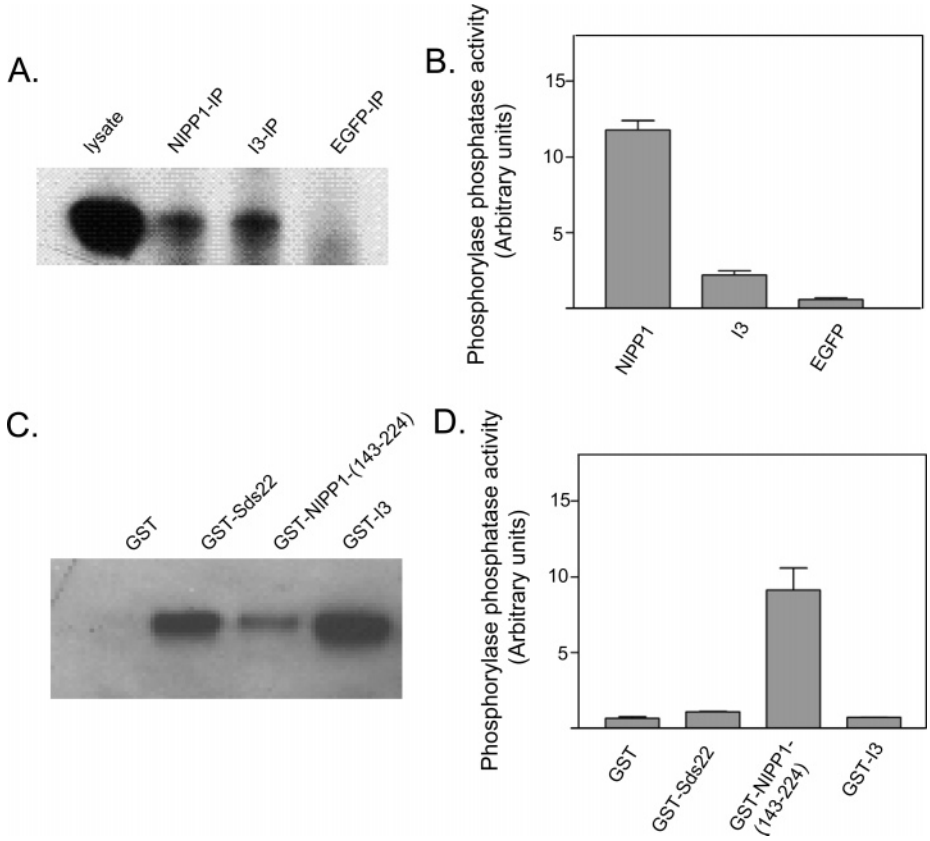

FIGURE 10: Freshly prepared lysates contain an inactive complex of Sds22, PP1, and I3. (A) COS1 cell lysates, prepared in the presence of 300 mM KCl to freeze the activation state of Sds22-associated PP1, were immediately used for immunoprecipitation with antibodies against NIPP1 or I3 and protein A-TSK. An EGFP antibody was added under the control condition. The immunoprecipitates were examined for the presence of PP1 by immunoblotting. (B) Aliquots of the same samples were used for the assay of the trypsin-revealed phosphorylase phosphatase activity. (C) COS1 cells were transfected with GST, GST−Sds22, GST−NIPP1-(143−224), or GST−I3. The GST fusions were pulled down from the cell lysates with glutathione agarose, and the pellets were analyzed for PP1 by immunoblotting. (D) The pellets were also assayed for trypsin-revealed phosphorylase phosphatase activity. The results in panels B and D represent means ± the standard error ($n = 3$).

can only speculate about its function. Perhaps I3 acts as an inhibitor of PP1 until it is transferred to its final destination. Alternatively, I3 may play a role in the nuclear targeting of PP1. Consistent with this notion, we have reported that PP1 has no functional nuclear localization signal and that its nuclear targeting is mediated by interactors with an RVxF motif (*15*). Indeed, unlike Sds22, I3 was able to target PP1 to the nucleus (*25*). Finally, we cannot exclude the possibility that I3 stabilizes the complex between Sds22 and PP1, as suggested by the much stronger interaction between Sds22 and PP1 in two-hybrid assays, following the coexpression of I3 (Figure 1B).

In conclusion, we have identified and characterized a mammalian complex of catalytically inactive PP1 that is sandwiched between the regulators Sds22 and I3. Our study paves the way for directed efforts aimed at elucidating the role and regulation of this ancient holoenzyme.

ACKNOWLEDGMENT

Nicole Sente and Karin Schildermans provided expert technical assistance.

REFERENCES

1. Bollen, M. (2001) Combinatorial control of protein phosphatase-1, *Trends Biochem. Sci. 26*, 426−431.
2. Ceulemans, H., and Bollen, M. (2004) Functional diversity of protein phosphatase-1, a cellular economizer and reset button, *Physiol. Rev. 84*, 1−39.
3. Janssens, V., and Goris, J. (2001) Protein phosphatase 2A: A highly regulated family of serine/threonine phosphatases implicated in cell growth and signalling, *Biochem. J. 353*, 417−439.
4. Ceulemans, H., Stalmans, W., and Bollen, M. (2002) Regulator-driven functional diversification of protein phosphatase-1 in eukaryotic evolution, *BioEssays 24*, 371−381.
5. Ohkura, H., and Yanagida, M. (1991) *S. pombe* gene sds22+ essential for a midmitotic transition encodes a leucine-rich repeat protein that positively modulates protein phosphatase-1, *Cell 64*, 149−157.
6. Hisamoto, N., Frederick, D. L., Sugimoto, K., Tatchell, K., and Matsumoto, K. (1995) The EGP1 gene may be a positive regulator of protein phosphatase type 1 in the growth control of *Saccharomyces cerevisiae*, *Mol. Cell. Biol. 15*, 3767−3776.
7. Garcia-Gimeno, M. A., Munoz, I., Arino, J., and Sanz, P. (2003) Molecular characterization of Ypi1, a novel *Saccharomyces cerevisiae* type 1 protein phosphatase inhibitor, *J. Biol. Chem. 278*, 47744−47752.
8. Peggie, M. W., MacKelvie, S. H., Bloecher, A., Knatko, E. V., Tatchell, K., and Stark, M. J. R. (2002) Essential functions of Sds22p in chromosome stability and nuclear localization of PP1, *J. Cell Sci. 115*, 195−206.
9. Pedelini, L., Marquina, M., Ariño, J., Casamayor, A., Bollen, M., Sanz, P., and Garcia-Gimeno, M. A. (2007) Ypi1 and Sds22 proteins regulate the nuclear localization and function of yeast type 1 phosphatase Glc7, *J. Biol. Chem. 282*, 3282−3292
10. Pinsky, B. A., Kotwaliwale, C. V., Tatsutani, S. Y., Breed, C. A., and Biggins, S. (2006) Glc7/protein phosphatase 1 regulatory subunits can oppose the Ipl1/aurora protein kinase by redistributing Glc7, *Mol. Cell. Biol. 26*, 2648−2660.
11. Ceulemans, H., Vulsteke, V., De Maeyer, M., Tatchell, K., Stalmans, W., and Bollen, M. (2002) Binding of the concave surface of the Sds22 superhelix to the α4/α5/α6-triangle of protein phosphatase-1, *J. Biol. Chem. 277*, 47331−47337.

12. Zhang, J., Zhang, L., Zhao, S., and Lee, E. Y. (1998) Identification and characterization of the human HCG V gene product as a novel inhibitor of protein phosphatase-1, *Biochemistry 37*, 16728−16734.
13. Wakula, P., Beullens, M., Ceulemans, H., Stalmans, W., and Bollen, M. (2003) Degeneracy and function of the ubiquitous RVXF motif that mediates binding to protein phosphatase-1, *J. Biol. Chem. 278*, 18817−18823.
14. Beullens, M., Vulsteke, V., Van Eynde, A., Jagiello, I., Stalmans, W., and Bollen, M. (2000) The C-terminus of NIPP1 (nuclear inhibitor of protein phosphatase-1) contains a novel binding site for protein phosphatase-1 that is controlled by tyrosine phosphorylation and RNA binding, *Biochem. J. 352*, 651−658.
15. Lesage, B., Beullens, M., Nuytten, M., Van Eynde, A., Keppens, S., Himpens, B., and Bollen, M. (2004) Interactor-mediated nuclear translocation and retention of protein phosphatase-1, *J. Biol. Chem. 279*, 55978−55984.
16. Beullens, M., Van Eynde, A., Stalmans, W., and Bollen, M. (1992) The isolation of novel inhibitory polypeptides of protein phosphatase 1 from bovine thymus nuclei, *J. Biol. Chem. 267*, 16538−16544.
17. Ceulemans, H., De Maeyer, M., Stalmans, W., and Bollen, M. (1999) A capping domain for LRR protein interaction modules, *FEBS Lett. 456*, 349−351.
18. Dinischiotu, A., Beullens, M., Stalmans, W., and Bollen, M. (1997) Identification of sds22 as an inhibitory subunit of protein phosphatase-1 in rat liver nuclei, *FEBS Lett. 402*, 141−144.
19. Bollen, M., and Stalmans, W. (1992) The structure, role, and regulation of type 1 protein phosphatases, *Crit. Rev. Biochem. Mol. Biol. 27*, 227−281.
20. Bollen, M., DePaoli-Roach, A., and Stalmans, W. (1994) Native cytosolic protein phosphatase-1 (PP-1S) containing modulator (inhibitor-2) is an active enzyme, *FEBS Lett. 344*, 196−200.
21. Connor, J. H., Weiser, D. C., Li, S., Hallenbeck, J. M., and Shenolikar, S. (2001) Growth arrest and DNA damage-inducible protein GADD34 assembles a novel signaling complex containing protein phosphatase 1 and inhibitor 1, *Mol. Cell. Biol. 21*, 6841−6850.
22. Eto, M., Elliott, E., Prickett, T. D., and Brautigan, D. L. (2002) Inhibitor-2 regulates protein phosphatase-1 complexed with NimA-related kinase to induce centrosome separation, *J. Biol. Chem. 277*, 44013−44020.
23. Eto, M., Kitazawa, T., and Brautigan, D. L. (2004) Phosphoprotein inhibitor CPI-17 specificity depends on allosteric regulation of protein phosphatase-1 by regulatory subunits, *Proc. Natl. Acad. Sci. U.S.A. 101*, 8888−8893.
24. Stone, E. M., Yamano, H., Kinoshita, N., and Yanagida, M. (1993) Mitotic regulation of protein phosphatases by the fission yeast sds22 protein, *Curr. Biol. 3*, 13−26.
25. Llorian, M., Beullens, M., Lesage, B., Nicolaescu, E., Beke, L., Landuyt, W., Ortiz, J. M., and Bollen, M. (2005) Nucleocytoplasmic shuttling of the splicing factor SIPP1, *J. Biol. Chem. 280*, 38862−38869.

BI7003119